AADE-18-FTCE-126

Advanced X-ray Technology for Real-Time High Pressure Mass Flow Rate Measurement

Vivek Singhal, Pradeep Ashok, and Eric van Oort, The University of Texas at Austin

Abstract

Accurately measuring mass flow rate in real-time at the well inlet where pressures can approach 7500 psi has remained elusive. Drilling contractors still primarily rely on the antiquated pressurized mud density cup and the pump stroke counter for this "measurement" of flow into the well. Gamma ray densitometer is a potential solution, but its use has been limited due to its radioactive source and slow response times. A metering technology that shows good performance is the continuously excited clamp-on transit time ultrasonic flowmeter. However, the meter accuracy is in a 95-99% range and deteriorates at low flow rates. Past efforts to commercialize low-cost / low-pressure x-ray technology, for use in downstream oil and gas, which is based on proven gamma ray principles have also been unsuccessful. However, advances in novel materials and measurement technologies are now making it possible for us to re-visit relatively low cost x-ray mass flow rate measurement systems. These systems can provide real-time mass flow rate (i.e. density and flow rate) measurements with 99% accuracy and 1 Hz frequency. This paper discusses how new x-ray technology can be used to make such higher frequency and high accuracy real-time mass flow rate measurements. Details of extensive lab measurements and considerations for field application will be shared in this paper. It is expected that the technology when implemented will be a step-change improvement in current delta flow (flow in – flow out) assessment and will positively contribute to early kick detection and managed pressure drilling control.

Introduction

High cost operations such as deepwater well construction can greatly benefit from higher accuracy and higher frequency inlet mass flow-rate measurements, particularly if measurement data can be obtained at an accuracy of 99% or greater and at a frequency of 1 Hz. Improved mass flow rate (density x volumetric flow rate (VFR)) measurements can lead to improved real-time estimation of delta flow rate, the difference between flow out and flow into the well, which is one of the primary indicators for trouble events such as kicks or lost circulation. An x-ray sensor can measure the density of the drilling mud and its VFR, which can then be used to calculate its mass flow rate. Improved density and VFR data allows for better control of the well bore pressure profile during static and circulating conditions. This improved characterization of the well bore pressure profile allows one to drill wells with narrow drilling margins without non-productive time, resulting in safer and more cost effective well construction operations.

X-ray technology shows great promise for mass flow measurements because it is based on the proven principles of gamma ray densitometry, which can measure density with greater than 99% accuracy. Recent advances in low density (~1.3 SG) and high pressure (>20 ksi) carbon reinforced polymers (CRPs) are making it possible to explore x-rays for these measurements. These CRPs offer a lower thickness-to-pressure ratio than the high density steel (~8 SG) currently used in standpipe construction. A sensor constructed from CRP material would allow for significantly greater x-ray transmission than steel, and thereby greatly reduce the voltage and power demand on the x-ray source. These lower voltage and power demands drastically reduce the cost, size, weight and complexity of the x-ray source, making it practical and safe for use in well construction applications.

Research towards developing x-ray sensor technology capable of measuring mass flow rate through a 4 inch CRP embedded pipe with mud density and VFR not exceeding 20 ppg (2.4 SG) and 1200 gpm respectively is presented in this paper.

We begin by discussing the experiments conducted to determine the minimum x-ray source voltage and power required by the sensor, in order to achieve x-ray penetration through the drilling mud (or other well construction fluid) and the CRP pipe. The two approaches that were explored to estimate density are then discussed. The first approach is an empirical approach where sensor gray level values are directly mapped onto mud density values determined from lab experiments. These mappings are then used in the field to estimate density. The second approach is a model-based approach that estimates density using the Beer Lamberts law. The explicit assumption in developing the two density methods is that the mud density is only changing due to influx of unwanted low gravity solids (LGS) from the formation. Changes from any other causes, such as temperature and pressure variation, addition and loss of weighing material, etc., require implementation of correction factors. Instances when these correction factors are needed are also discussed.

Preliminary results are presented from testing of an algorithm that was developed to investigate if digital video of tracer particles, introduced into the circulating fluid, contains

sufficient information to interpret fluid velocity with greater than 99% accuracy. Digital video is used for investigation since experiments using digital images are much easier to perform than using x-ray radiographs. Upon successful testing of this algorithm, software will be developed that can measure velocity from x-ray radiographs. Results are also shared from an experiment designed to evaluate the capability of commercial imaging detectors to detect high speed tracers.

X-Ray Source Power Requirements

The proposed x-ray sensor consists of a steel spool piece which connects to the standpipe using a pressure tight seal. It also serves as the housing that contains the CRP pipe and mounting provisions for the x-ray source and detector. In this work, we will consider a polychromatic x-ray energy source given its lower cost, size and complexity compared with the monochromatic energy source. A polychromatic energy source generates x-rays ranging from 0 eV to the maximum source energy, as opposed to a monochromatic energy source which primarily generates x-rays of a single energy. The x-rays lose energy as they propagate through the pipe and the drilling mud, a process known as x-ray attenuation. For the application discussed in this paper, it is observed that the Beer Lamberts law (Eq. 1) serves as a good approximation for determining the attenuation of polychromatic energy x-rays.

$$I = I_0 * \exp\left(\sum_{\substack{material \\ type}} -\mu_m \rho d\right) \qquad 1$$

Where I is x-ray intensity incident on the detector after attenuation by sample in its path (gray level value), I_0 is the x-ray intensity incident on the detector after attenuation by air (gray level value), μ_m is the mass attenuation coefficient of the homogeneous sample (cm^2/g), ρ is the density of the homogeneous sample (g/cm^3), and d is the sample thickness (cm).

It is noted that mixtures consisting of two different constituent compounds can have the same density. However, the x-ray attenuation of these two mixtures will be different due to differences in their mass attenuation coefficients.

Little to no change is observed in the 'I' value in Eq.1 with changes in drilling mud properties unless the x-rays have sufficient voltage (kV) and power (W) to penetrate the sample. The path taken by the x-ray beam in the proposed sensor, from the source to the detector, is schematically shown in Figure 1. The x-rays pass through some air gaps, the CRP pipe, a low density liner material used to protect the CRP pipe from the abrasive mud, and the drilling mud itself. The maximum expected widths for the various components that the x-ray beam must penetrate is shown in Figure 1, along with the maximum angle the x-ray beam is expected to make with the source and detector centerline. Ignoring attenuation by air, Figure 1 shows that the x-rays need to penetrate 8 inches of material to alter the gray level (GL) value of the pixel in its path.

For the detectors used in the experiments, the GL value for a given pixel is around 65000 when it is not exposed to x-rays. This GL value can fluctuate by approximately 200 due to inherent design limitations of the detector. Thus, for a detector placed in the path of x-rays and showing a change in pixel value of greater than 200 GL's, it can be stated with a high level of confidence that the resulting change is due the x-ray penetration through the sample placed between the x-ray source and the detector.

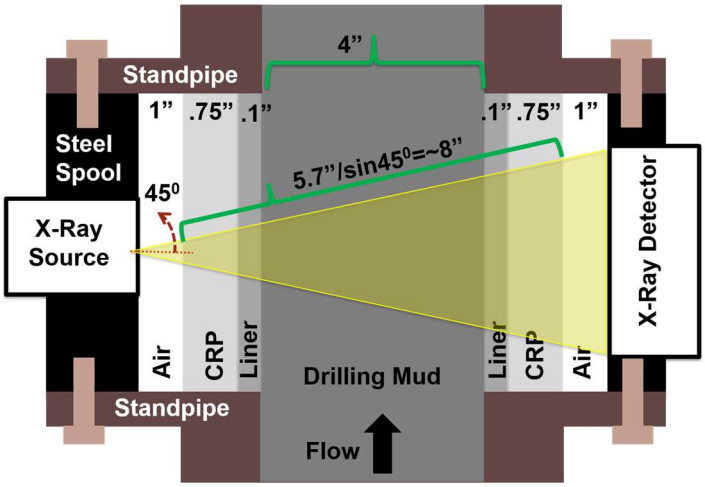

Figure 1: Path of x-ray beam from source to detector.

The following experiment was conducted to determine the minimum x-ray kV and W required to penetrate the 20 ppg mud inside the CRP pipe. For this experiment, the entire system in Figure 1 was simulated using an 8 inch plastic pipe filled with a water based mud weighted with hematite (5.3 SG) and 10% by volume concentration of LGS (2.5 SG) resulting in a total mud weight of 22 ppg (~2.6 SG). Hematite was used because it has a higher density in comparison to other commonly used weighing agents. Therefore, the volume of hematite required to formulate a given density mud was lower, which made it easier to mix using the available lab equipment. The CRP pipe and the liner were also simulated by the formulated mud since the mud had a higher density and effective atomic number compared to the CRP pipe and the liner and therefore resulted in greater attenuation of x-rays.

The x-ray attenuation experiments with the 8 inch plastic pipe were conducted using a source with a maximum power rating of 1500 W and maximum voltage rating of 450 kV. It was determined that the minimum voltage required to achieve x-ray penetration through the 8 inch pipe at the 1500 W rating needs to be 320 kV.

Experiments show that the source power requirement for x-rays to penetrate a fixed sample size increases with decreasing source voltage. The experiments to demonstrate the source power verses voltage relationship were conducted using a 5 inch and an 8 inch plastic pipe. These are not to be confused with the 8 inch plastic pipe in Figure 1 that was used to simulate the sensor.

Power requirements at high voltage settings for the 5 inch plastic pipe filled with 22 ppg water based mud weighted with hematite and 10% by volume concentration of LGS (2.5 SG) are shown in Figure 2. Power requirements at low voltage settings for the 8 inch plastic pipe filled 11.5 ppg water based mud weighted with hematite are shown in Figure 3.

It can be observed from Figure 2 that for voltages and powers tested in the experiment, the two quantities follow an almost linear relationship above a threshold voltage level. Below this threshold voltage power requirement increases exponentially with reducing voltage levels. The linear relationship between power and voltage is also shown in Figure 3.

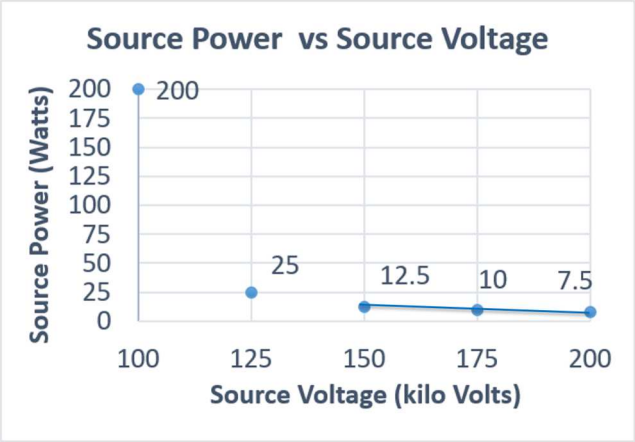

Figure 2: Power vs Voltage for a 22 ppg mud in a 5-inch plastic pipe.

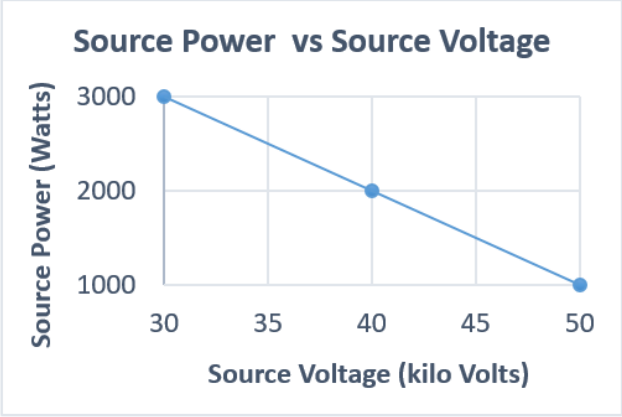

Figure 3: Power vs Voltage for a 11.5 ppg mud in an 8-inch plastic pipe.

Source voltage and power directly impact cost, size, weight and complexity of x-ray equipment. For a source voltage greater than 450 kV, using x-rays for mass flow measurements becomes impractical due to a significant increase in these parameters. X-ray tube pricing generally increases with voltage rating. For example, budget pricing by an x-ray tube supplier shows that x-ray tube pricing doubles from $8,000 to $16,000 when going from 225 kV to 350 kV (pricing as per the time this paper was written). The price again doubles to $32,000 when selecting a 450 kV tube. The maximum power rating available for the 225/350/450 kV tubes is 3000/4200/4500 W respectively. The price for the generator that powers the x-ray tubes follows a similar trend in pricing increase with increasing source voltage.

To minimize procurement cost of the x-ray source to be used in the sensor, it is desirable to minimize source voltage and maximize power. Thus, it is recommended that x-ray penetration for the 8 inch plastic pipe used to simulate the sensor as shown in Figure 1 be verified at 225 kV using a 3000 W source as well. If x-ray penetration is observed at 225 kV/3000 W, then the 225 kV/3000 W source should be chosen in favor of the 350 kV/1500 W source.

Density Estimation Methods

Two methods, an empirical method and a model-based method, were developed in order to estimate density. With these methods, real time density measurements with an accuracy of 99% or greater and a measurement frequency of 1 Hz are feasible, on the high pressure standpipe. The test setup used to conduct the experiments to develop these density estimation methods is shown schematically in Figure 4. The test setup ensured that the distance of the test samples was fixed relative to the source and the detector for each x-ray exposure. The stage in the test setup was fitted with grooves to enable exact alignment over various experimental runs. The depth of the sample bottles was 1 inch and the width and height were approximately 2.5 inches each. An x-ray source voltage of 100 kV and source power of 44 W were used in the experiments. The exposure time was set to 1 second (i.e. 1 Hz frequency). A sample radiograph obtained from the experimental setup is shown in Figure 5. Quantities I0 and Imud were measured by averaging all the gray pixel values to a single GL value across windows 1 and 3 respectively (Figure 6). Units of intensity ‘I’ are therefore expressed in GL value units.

Glycerol and water samples shown in the test setup were used for calibration purpose. Real-time calibration of the x-ray system is necessary to ensure repeatability and accuracy of density measurements. Details on how this calibration was performed is outside the scope of this paper. Furthermore, all density experiments were conducted under static conditions at standard temperature and pressure. However, in the standpipe the fluid is flowing and is subject to temperatures and high pressure variations. The effect of the fluid flow rate, temperature and pressure on x-ray attenuation has been investigated and will be reported on elsewhere.

For experimental evaluation of the empirical and model-based methods, three base muds composed of water (solvent) viscosified with Xanthan Gum and weighted with hematite (5.3 SG) were used. Water was the solvent and hematite was used as weighting material, indicated as high gravity solid (HGS). The densities of these base muds were 9.03, 9.51, and 9.95 ppg respectively and are shown in Table 1. LGS (2.5 SG) were then added to these base muds.

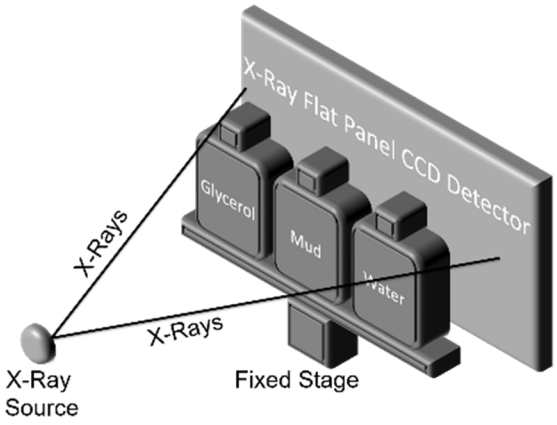

Figure 4: Experimental setup.

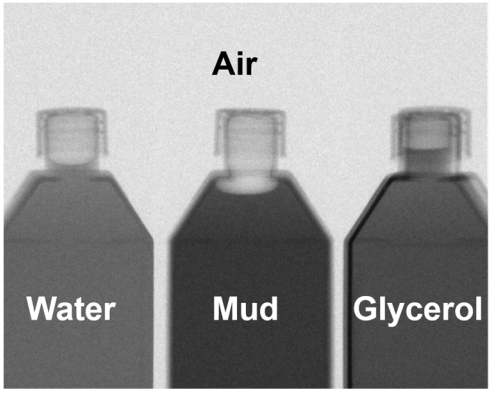

Figure 5: Sample radiograph of test setup.

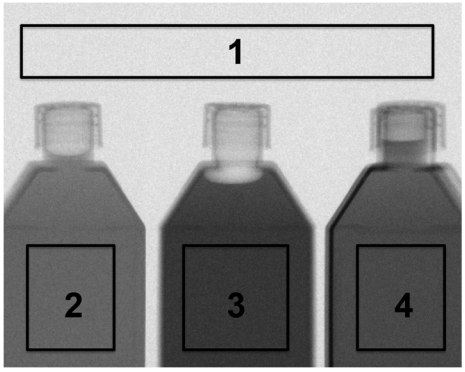

Figure 6: Gray level windows.

The LGS concentration was varied between 0 and 8%, which approaches the maximum % LGS that are typically permitted in a water-based mud system. Allowing the % LGS to increase beyond this level can cause negative effects on fluid viscosity, gel strength and fluid loss control. The final mud densities upon addition of LGS are shown in Table 1. These densities were measured using a standard API density cup. The two methods, and the results from the validation of these methods, are discussed below.

Table 1: Drilling mud density and composition used for experimental evaluation of the density estimation methods

Test Matrix for Drilling Mud with LGS			
Sample #	Base Mud Density (ppg)	% LGS by Volume	Final Measured Density (ppg)
1	9.03	0	9.03
2	9.03	1	9.15
3	9.03	4	9.50
4	9.03	8	9.92
5	9.51	0	9.51
6	9.51	1	9.65
7	9.51	3	9.86
8	9.51	6	10.19
9	9.95	0	9.95
10	9.95	1	10.11
11	9.95	4	10.46
12	9.95	8	10.85

Empirical Method

In the empirical method, sensor GL values are directly mapped onto mud density values through in lab experiments. These mappings can then be used in the field to estimate density. The goal of the experiments was to determine the minimum density interval at which to collect GL values in the lab, so as to ensure greater than 99% in-field estimation accuracy. Experimental data shows that data points collected at 1 ppg density intervals, represented by the four corners of the GL tracks shown in Figure 7, were adequate for mapping and thereby estimating the density of unknown mud samples with an accuracy of 99% or greater. The mappings were used to create a lookup table, which was generated by dividing the plot in Figure 7 into 50x50 bins along the tracks of increasing HGS and LGS respectively.

In order to use the empirical method, the initial density of the mud needs to be measured using the mud density cup. This density measurement, along with the corresponding GL reading from the x-ray detector, is then used to find the position of the mud in the lookup table. The density of the mud will then continue to change in the direction of increasing LGS (a result of entrainment of drilled solids). The new density can be determined in real-time by searching for any subsequent change in GL value and its corresponding density value in the lookup table.

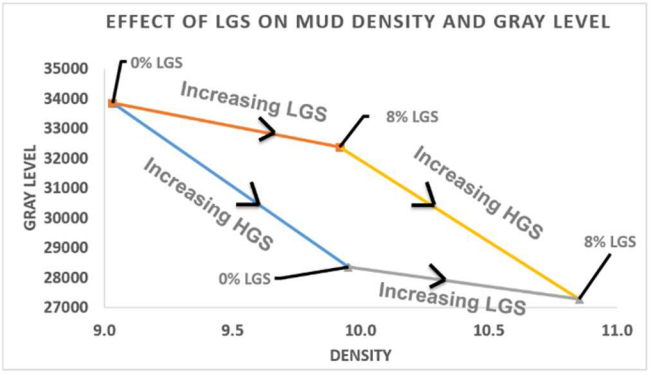

Figure 7: Effect of LGS and HGS on mud density and Gray Level.

Model Based Method

Unlike the empirical method which uses lookup tables, the model-based method relies on the Beer Lambert's law to estimate mud density based on field GL values. The LGS density is pre-known as it can be estimated from formation core samples and other geological data. The mass attenuation coefficient of LGS can also be pre-determined experimentally in the lab. A detailed procedure to determine the mass attenuation coefficient of the LGS is outside the scope of this paper. The initial density of the mud is measured using a standard API density cup. The mass attenuation coefficient for the mud is then calculated using:

$$\mu_{mud} = -\ln\left(\frac{I}{I_0}\right)/\rho_{mud}\mathrm{d}_{mud} \qquad 2$$

Upon ingress of LGS into the mud, its new density can be determined from Eqs. 3, 4 & 5. There are three unknows between the three equations, i.e., the new mud density and the proportions of the mud and the LGS in the 1 inch deep plastic bottle (representative of the fixed diameter stand pipe). Equations 6 & 2 are then used to calculate the new mass attenuation coefficient of the mud. As more LGS gets entrained in the mud, Eqs. 2 through 6 can be used recursively to measure the mud density in real-time. The estimation errors using the model based method show an error bound between +0.72% and -1.17% with a median value of 0.15%.

$$\mathrm{I} = \mathrm{I}_0\exp - \left(\mu_{\mathrm{m\_mud}}\rho_{\mathrm{mud}}\mathrm{d}_{\mathrm{mud}}+\mu_{\mathrm{m\_LGS}}\rho_{\mathrm{LGS}}\mathrm{d}_{\mathrm{LGS}}\right) \qquad 3$$

$$\mathrm{d}_{\mathrm{ID}} = \mathrm{d}_{\mathrm{mud}} + \mathrm{d}_{\mathrm{LGS}} \qquad 4$$

$$\rho_{mud\_new} = (\rho_{\mathrm{mud}}\mathrm{d}_{\mathrm{mud}} + \rho_{\mathrm{LGS}}\mathrm{d}_{\mathrm{LGS}})/\mathrm{d}_{\mathrm{ID}} \qquad 5$$

$$\rho_{mud} = \rho_{mud\_new} \qquad 6$$

Comparison of Density Estimation Methods

The empirical method is the preferred method when the LGS are well-characterized (for example when drilling duplicated wells in the same formation) and the relative proportion of the weighing agent and the solvent in the mud remain constant. For all other cases, the model-based method is the preferred method. This is because adjustments to mass attenuation coefficients and density values can easily be made in the model based method to compensate for changes in the LGS composition or changes in relative proportion of the weighing agent and the solvent. The model can also be corrected by adjusting the mass attenuation coefficient and density values, in case discrepancies are noticed between measured and estimated values. For the empirical method, for which the data is collected experimentally in the lab, these correction factors are more difficult to implement.

Volumetric Flow Rate (VFR) Measurement

Density is one of the two variables required in measuring drilling mud mass flow rate through the high pressure standpipe. The second variable is the VFR of the mud. VFR can be estimated by multiplying the known cross-sectional area of the standpipe with the mud velocity, which can be as high as 30 ft/sec. A non-invasive method, due to the abrasive nature of drilling muds, to measure this velocity is desirable, and has been pursued for many years now. A method proposed here, to estimate mud velocity, uses information from the radiographs of tracer particles that are intentionally introduced into the drilling mud. These tracer particles need to be designed such that they do not interfere with existing drilling processes and can seamlessly work with existing drilling equipment. The x-ray equipment needs to have the capability to image these high speed tracers with a contrast level that can be identified by a computer based algorithm. Most importantly, the 2D radiographs of tracer particles should contain sufficient information to measure mud velocity with greater than 99% accuracy. This section discusses the progress and future work related to the development of this method.

VFR using Digital Images

Experiments to investigate if 2D images of tracer particles contain sufficient information to interpret mud velocity with greater than 99% accuracy were conducted using digital video techniques. Experiments with digital video are much easier to perform as compared to using x-ray radiographs. Flow experiments with x-rays can be very time consuming and expensive. It can be difficult to locate and schedule with test labs that have adequate resources to conduct the x-ray experiments. Furthermore, the flow loop needs to be moved to the test lab for each of the many experimental runs.

An algorithm was developed to estimate fluid velocity from the captured 2D videos of tracer particles. The algorithm uses block matching (Figure 8) to determine the relative motion of tracers between two subsequent images of fluid flow. The image at the earlier time instance is referred to as the reference frame, and the one at a latter instance in time as the current frame. To implement block matching, the reference frame is divided into blocks (4x4 pixels in size for example). The best match for each block is then located in the current frame. The match is performed using an Advanced Rood Pattern Search (ARPS) described in detail by Barjatya et al., (2004). A vector, representing the displacement, is drawn between the matching

elements. The horizontal component of the vector represents displacement in the horizontal direction or direction of flow. The non-zero horizontal displacements, representing areas where tracers are detected, are averaged over each frame to give an average displacement in pixels per frame. This average displacement is then divided by the frame rate to get the average fluid velocity in pixels per second. The velocities can be time averaged over multiple frames to get average fluid velocity over longer time intervals (1 Hz for example). If the number of pixels per unit distance of the pipe section being imaged is known, the velocity can be converted from pixels per second to distance per second.

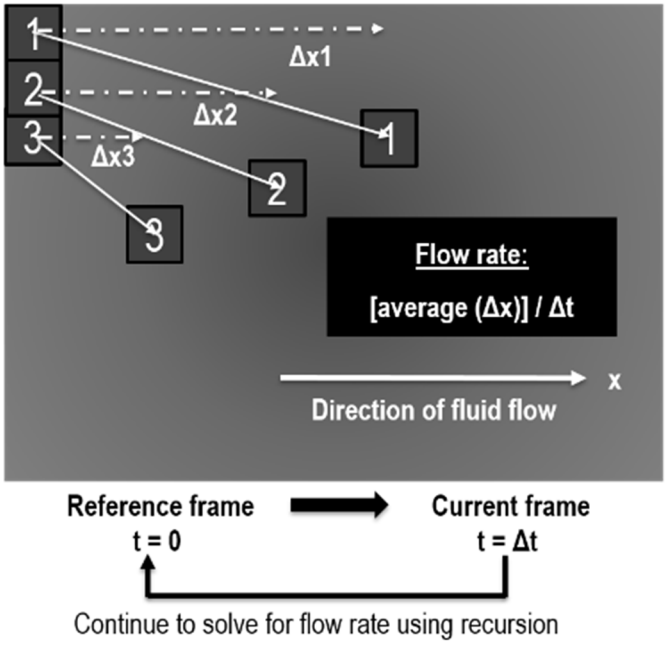

Figure 8: Schematic representation of the block matching technique (Note: Figure is used for explanation purposes only and is not to scale).

Preliminary validation of the algorithm was conducted using a video of a fluid flowing through a transparent pipe and containing entrained air bubbles. The entrained air bubbles are used as tracers and the video is captured at thirty frames per second. One image of the fluid flow is shown in Figure 9. Displacement was calculated to be at 7 pixels/frame or 210 pixels/second. For a 1 foot pipe section with a 2 inch diameter, this would equate to 5 gpm. Visual inspection and a timer were used to confirm the velocity measurements. The algorithm shows good tracer detection and tracking capability. Future experiments are planned to validate the algorithm.

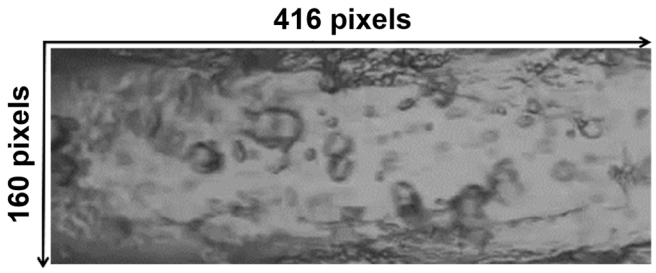

Figure 9: Image of fluid-flow used for preliminary testing.

Evaluating X-ray Detector Capability to Image High Velocity Tracers

Tungsten carbide (SG 15.3) beads/tracers (Figure 10 (b)) ranging in sizes and velocities as shown in Figure 10 (c) were imaged using a flat panel detector at 200 kV and 460 W. As can be seen in Figure 10 (a), the images were obtained with good contrast for bead numbers 1 through 5. The experiment demonstrates that the x-ray detectors are capable of detecting tracer particles, 6 mm in size, travelling at pipe velocities of up to 23 ft/sec. A subsequent experiment is planned to image tracers at relatively higher velocities.

It remains to be seen if sufficient contrast can be achieved when the tracers are entrained in a high density drilling mud in the 4 inch CRP sensor pipe. Tests need to be conducted with tracers (other than tungsten carbide) that are more representative of what could be used in the field.

Tracer contrast can be improved if needed by reducing the standpipe diameter, which could also result in reduced source voltage and power. However, this would lead to an additional pressure loss that must be overcome by the mud pumps. Furthermore, there will be an increase in tracer velocity which will require re-testing for x-ray detector capability at velocities greater than 30 ft/sec. These trade-offs will have to be carefully evaluated to optimize between pipe size, sensor performance, and system and energy costs.

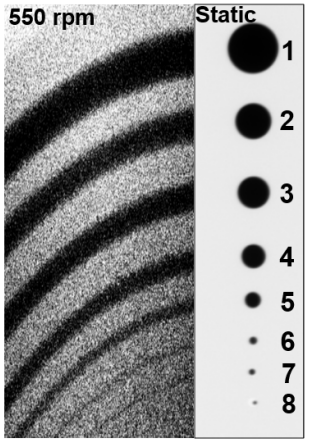

Bead #	OD (mm)	Distance from Rotational Axis (in)	Velocity (ft/sec)
1	6	4.7	23
2	5	4.4	21
3	4	4.0	19
4	3	3.8	18
5	2	3.5	17
6	1	3.3	16
7	.8	3.1	15
8	.5	3.0	14

(a) (b) (c)

Figure 10: (a) Radiograph of moving tracers (b) Radiograph of static tracers (c) Tracer test matrix.

Conclusions

Main conclusions from this project are:

- Carbon reinforced polymers make x-ray application practical and safe for density and flow rate measurements in the high pressure standpipe.
- X-ray source voltage and power required to achieve penetration through a given sample follows a linear relationship between certain voltage values. Below the lower end of this voltage threshold, power requirement increases at an exponential rate.
- Drilling mud density measurements can be made at greater than 99% accuracy at 1 Hz measurement frequency with both empirical and model-based methods.
- X-ray detectors are fast enough to detect objects as small as a 0.25-inches moving at velocities up to 23 ft/sec.
- Imaging of tracers entrained in a fluid shows good potential for making volumetric flow rate measurements with greater than 99% accuracy and 1 Hz measurement frequency.

Acknowledgments

The authors would like to thank Weatherford International for funding this research, and for their technical guidance during project execution.

Nomenclature

d = *sample thickness, cm*
d_{ID} = *depth of sample bottle, cm*
d_{LGS} = *proportion of LGS in sample bottle, cm*
d_{mud} = *proportion of mud in sample bottle, cm*
eV = *electron volt*
GL = *gray level*
gpm = *gallons per minute*
I = *x-ray intensity pre-attenuation by sample, GL*
I_0 = *x-ray intensity post-attenuation by sample, GL*
I_{mud} = *x-ray intensity post-attenuation by mud, GL*
KeV = *kilo electron volt*
ksi = *kilo pounds per square inch*
KV = *kilo volt*
ppg = *pounds per gallon*
rpm = *revolutions per minute*
SG = *specific gravity*
t = *time, seconds*
W = *watt*
Δt = *time interval, seconds*
ρ = *density, g/cm3*
ρ_{mud} = *density of mud, g/cm3*
ρ_{LGS} = *density of LGS, g/cm3*
ρ_{mud_new} = *new mud density, g/cm3*
μ_m = *mass attenuation coefficient, cm2/g*
μ_{m_mud} = *mass attenuation coefficient of mud, cm2/g*
μ_{m_LGS} = *mass attenuation coefficient of LGS, cm2/g*

Glossary

VFR = *Volumetric Flow Rate*
CRP = *Carbon Reinforced Polymer*
LGS = *Low Gravity Solid*
HGS = *High Gravity Solid*

References

1. Sanderson, M. L., & Yeung, H. (2002). Guidelines for the use of ultrasonic non-invasive metering techniques. Flow measurement and Instrumentation,13(4), 125-142.
2. Tjugum, S. A., Frieling, J., & Johansen, G. A. (2002). A compact low energy multibeam gamma-ray densitometer for pipe-flow measurements. Nuclear Instruments and Methods in Physics Research Section B: Beam Interactions with Materials and Atoms, 197(3), 301-309.
3. Tjugum, S. A. (2010). U.S. Patent Application No. 12/902,473.
4. Stephenson, K. E., & Becker, A. J. (1997). U.S. Patent No. 5,689,540. Washington, DC: U.S. Patent and Trademark Office.
5. Barjatya, A. (2004). Block matching algorithms for motion estimation. IEEE Transactions Evolution Computation, 8(3), 225-239.